E14-2003-24

S. A. Karamyan, F. Grüner*, W. Assmann*

COOLING AND HEATING OF THE ION FLUX ON THE TRANSMISSION THROUGH CRYSTALS

Submitted to the Proceedings of the Japan–Russia Symposium
on Interaction of Fast Charged Particles with Solids,
November 2002, Kyoto, Japan

*Sektion Physik, Ludwig-Maximilians Universität München, Garching,
D-85748, Germany

1. Introduction

1.1. Crystal response to ion flux

As is known more than a century, atoms in the monocrystalline medium form the highly symmetric solid lattice characterized by the long-range ordering. The equilibrium position of an atom corresponds to the rather shallow potential minimum, and a high stability of the structure could not be predicted, especially at strong perturbations created by the charged particle beam. However, the soft structure unexpectedly demonstrates in many cases the resistivity to the strong impact of energetic particles. First model invented by Kinchin and Pease [1] identifies the lattice defects after irradiation as atoms displaced in elastic collisions. Later, such model have been developed and improved very much, and the Monte Carlo codes, like TRIM, are available today. They take into account the fate of all colliding encounters, the cascade multiplication of defects, energy losses and many other details. But, in principle, the fundamental process is still a scattering of fast projectiles and crystal atoms. It was clear that the bulk of energy released by projectile is transferred to electrons in inelastic collisions, not directly to the displaced atoms. After the discovery of giant, linearly extended defects – tracks in solids – it was realized that in some cases the energy deposited into the electronic subsystem plays a dominating role for crystal damage. The threshold behavior of defectness versus the electronic stopping parameter $(dE/dx)_e$ is typical for the case of track-sensitive materials.

The model of Coulomb explosion was proposed 40 years ago, Ref. [2], for explanation of the mechanism of ions acceleration after electrons release. More complicated schemes are discussed in Refs. [3-5] and a role of electronic stopping for sputtering was clearly demonstrated. Correlation between track formation and sputtering yield has been discussed. Many peculiarities for different materials are experimentally observed. In most sophisticated cases even interference between effects created by electronic and nuclear stopping are described. But, in general, the scheme was still relatively simple: the swift projectile produced defects due to the energy deposition to electronic and nuclear subsystems of the crystal. The thermal spike model, Refs. [6,7], has been developed and in some discussions it is considered as an alternative option to the Coulomb explosion model. But it is clear that they describe different stages of the process in time. Coulomb explosion is responsible for the acceleration of atoms, means for the transmutation of the ionization energy to the kinetic energy of atoms. The thermal spike should be created after Coulomb explosion, and then the relaxation follows due to the evolution of spatial distribution of temperature near track. Such view on

the accomplishing role of Coulomb explosion and thermal spike has been directly formulated in Ref. [8], and recently this idea is quantitatively developed by the calculations of Ref. [9].

It was clear that electronic energy losses may produce no defects in some samples (mostly metals) or create tracks and giant sputtering in others (mostly insulators). But in addition, the annealing of defects because of high $(dE/dx)_e$ value have been revealed in Refs. [10,11] for semiconductors. The annealing due to a macroscopic temperature rise under the high-power beam was known earlier. In our case [10,11] the temperature rise in sample was insignificant, thus the processes within individual track should be important. At moderate temperature in thermal spike, the evaporation of material or shock-waves generation are not happening, while the thermal recrystallization takes place, like the recrystallization induced by powerful laser pulse. Finally, the crystal is recovered, even the atoms displaced due to the elastic collisions are incorporated again into the lattice at right locations. The slightly damaged structure is conserved up to high doses of Xe ions at 115 MeV in Ge, GaP and Si crystals. The threshold behavior of the recrystallization rate versus $(dE/dx)_e$ was confirmed [10,11].

The same threshold dependence may be observed not only for track formation, sputtering yield, recrystallization but also for some new effects, like fast diffusion, elemental mixing, chemical reactions and phase transformation, as is discussed recently, for instance in Ref. [12].

Until this point, only the features observed for monocrystalline materials have been of interest. Some processes can be very different when happen in polycrystalline and amorphous samples. Indeed, assume that the recrystallization takes place in some semiconducting crystal, and it leads to recovering of the lattice, means to the damage annealing. But the recrystallization in amorphous sample of the same compound means is, in definition, some sort of the disordering in the structureless material. So that, the damage discussed in Refs. [13-16] is not the same, maybe even opposite in essence in respect to the damage of crystals. Despite that, some correlation between the behavior of monocrystalline and amorphous materials may exist, and the very different manifestations are possible too. For instance, the formation of tracks in amorphous Si and graphite had been detected in Ref. [13], while no indication of the track creation in monocrystalline Si and diamond was found in many other investigations.

The damaging response of any sample depends strongly on the electronic and nuclear stopping power of the projectile, on the temperature, chemical species, macroscopic properties and structure of the sample. Such multiparameter dependence leads to the great variety of the manifestations. Thus, experimental studies in this field should be continued, while a lot of results had already been reported in literature. At section 2, we are going to throw more light on the interesting relation between damage and annealing in semiconducting crystals. Other sections of this article are devoted to a new phenomenon of crystal-induced peculiarities in flux distribution. So that, some introductory words should be told on this problem as well.

1.2. Ion-flux response to the transmission through crystal

Correlated multiple scattering of charged particle by the system of ordered atoms generates the outstanding series of effects called, in general, "channeling" in crystals. Experimentally, the channeling and blocking effects were discovered as late as on mid 1960-th, despite some initiating remarks had been known since the pioneering discussions in Refs. [17-19]. The discovery happened so late, obviously, because no one could expect that gentle collisions with screened atoms produce a significant effect. However, the small-angle deviation is regularly multiplied in the series of spatially correlated collisions and a noticeable effect can be easily observed. The basic properties of channeling and blocking were studied mostly using protons and α-particles as projectiles and the appropriate review could be found in Ref. [20].

Many unclear points have been still remaining about the channeling of heavy projectiles, because the charge exchange and other processes with electrons become to be important and may produce a new peculiarities. The approximation of elementary charge is no more valid for the heavy ion due to its composite structure, and the prevailing theory of channeling may be fail in this case. In the seminal theoretical work on channeling, Ref. [21], a reversibility rule was introduced being the consequence of time-reversibility for any trajectory of potential motion. The reversibility of angular dependencies of the yield in channeling and blocking conditions was shown in approximation of the multiple scattering

absence. Then, reversibility has been extended in Ref. [22] to the case of multiple scattering without damping, while the violation have corresponded to the presence of damping. The attempt to generalize the reversibility even to the case of damping is described in Ref. [23] using some concrete version of the multiple scattering model.

In experiments on detection of the crystallographic images for heavy ions scattered in monocrystalline targets [24,25], the transformation of blocking minima to channeling maxima was unexpectedly observed for ions emitted from deep layers in the crystal. Such transmutation of the trajectory type means the violation of the reversibility rule because in theory the rate of de- and re-channeling should be the same. Reversibility requires also that an initially isotropic flux will remain isotropic after transmission through a crystal. The geometry of isotropic flux was realized in experiments [26] and immediately the formation of channeling peaks was found and in some cases (at lower energy) the transformation of peaks to dips along crystallographic directions. Later, more detail measurements have been performed using protons [27], α-particles [28] and heavy-ions [29] transmitted through Si, Ni and Pt monocrystalline foils. Abundant pattern has been obtained, and the necessity to create a new model explaining the violation of reversibility becomes urgent.

In Ref. [26], the idea was introduced that the electron capture and loss processes are responsible for the observed cooling and heating of trajectories. We use "cooling" to indicate the appearance of enhancement and "heating" – the reduction of flux near crystalloghraphic direction because they correspond either to decreasing or to increasing of the transverse momentum, respectively. In Ref. [27], some qualitative predictions of the charge-exchange model are discussed, in particular, it is realized and experimentally confirmed that at high velocities, when the projectile is completely bare in crystal, such mechanism is switched off. In more details the model is developed and analyzed in Ref. [30]. After the brief review given above for the problems of our interest, let us to proceed with a presentation of concrete experimental results.

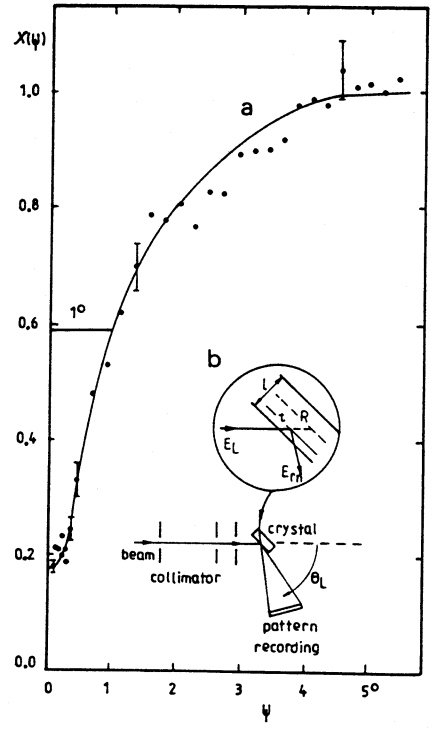

Fig.1. a) Profile of the blocking minimum detected for carbon recoils at irradiation of diamond target by 122 MeV Xe ions;
b) Scheme of the experiment.

2. Damage and annealing

Series of experiments have been carried out at Joint Institute for Nuclear Research, Dubna on the recording of crystallographic images formed at the detection of the scattered ions and recoils in the reflection geometry. Solid-state track detectors made of glass and polymers have been used, they allow to visualize the pattern after etching provided the density of tracks is high enough. The quantitative measurements of angular distributions of scattered particles near axes or planes of the monocrystalline target could be obtained by the detector scanning and counting of the track density.

There is shown in Fig.1 the blocking minimum profile observed under the detection of C recoils at θ_L=74° in irradiation of the diamond target by Xe-ion beam at 122 MeV. Also the sketch of the

experimental geometry is given there. In reflection geometry, the active layer thickness, t can be calculated taking into account the known energy of ejectile in lab. syst., energy losses of both projectile and ejectile and the detection threshold. Typically, thickness t, ion range R, and crystal thickness ℓ satisfy the inequality: $t << R << \ell$. So that, the detected blocking pattern characterizes the quality of crystal near the surface within a few μm thickness. At energies below Coulomb barrier, only products of Rutherford scattering are detected because nuclear reaction yield is suppressed. Large-angle scattering, $\theta_L > 30°$ and well defined depth distribution of scattered particles make sure that a high-quality blocking dip (like shown in Fig.1a) should be observed, and it is in fact detected at lowest doses of irradiation in all cases.

At the described conditions, many crystals were irradiated with the detection of the blocking profile as a function of fluence within the range from 10^{13} up to 10^{16} ions/cm^2. Polished (111)- or (110)-oriented crystal plates of 1 mm thickness were exposed under non-aligned conditions at room temperature. Beams of ions from C to Xe were used. After passing the collimator, the beam had the following parameters: an angular spread <0.5°, a diameter of 1 mm, and a pulsed power <1 W. The temperature rise under the beam was insignificant. Degrading of the blocking-pattern contrast and corresponding growth of the minimum yield χ_m at the center of dip clearly demonstrate the lattice damage with the increased fluence, Φ. Experimentally measured functions χ_m (Φ) have been recalculated and the defect concentration functions n_D (Φ) have been deduced. The method of such processing is described in Ref. [31], it involves the yield of scattering on displaced atoms and the dechanneled fraction on the transmission through the damaged layer.

At Dubna series of experiments the diamond, Si, Ge, GaP and W crystal were studied. Defectness of W as a function of dose and ion species can be reproduced within some standard calculations being proportional to a number of displaced atoms. Diamond irradiations showed also regular growth of the defect concentration with fluence. However, the damaging rate induced by Ar-ion irradiation was higher than that by Xe beam, unlike to the prediction of theory. Obviously, some rate of Frenkel-pair recombination is created in diamond by Xe beam, as well.

Most unusual behavior was revealed for the semiconducting crystals: Si, Ge, and GaP. The n_D (Φ) functions at high fluences of very heavy ions, like Xe, I are saturated at low level of the defect concentration, as shown in Fig.2 for Ge. The deviation from the standard theory prediction is as strong as by order of magnitude. Not only the saturation is observed. Even at low doses, the rate of defect production $dn_D/d\Phi$ by Xe ions is lower than for lighter ions. This can be explained only assuming the annealing of defects due to the high density of energy released by very heavy ion in electronic subsystem. Roughly speaking, defects generated in elastic collisions survive in the case of Ar ions, but they are annealed in the thermal spike created near the Xe-ion track. The temperature in the spike at this case is not enough to create a giant destruction similar to the latent track in insulators, but microheat near the ion trajectory is effective for the defect recombination. The same behavior was found for Ge, GaP and Si crystals.

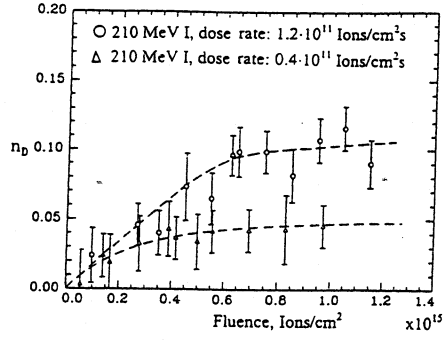

Fig.2. Defect concentration versus dose taken for 210 MeV I-ion beam irradiation of the Ge crystal. Dose rate effect is also clearly manifested.

The series of experiments with Ge has been performed also in München University [31] and the decreased damaging power of very heavy ions has been reproduced. In Fig.3 the relative damaging efficiency of ions in Ge crystal is shown as a function of the electronic stopping parameter $S_e = (dE/dx)_e$. The damaging efficiency is defined as the experimentally determined $dn_D/d\Phi$ derivative

at low fluences taken in ratio to the same parameter predicted by code TRIM. For heaviest ions this ratio reaches low value, like 0.03, means the annealing effect of electronic stopping is really strong.

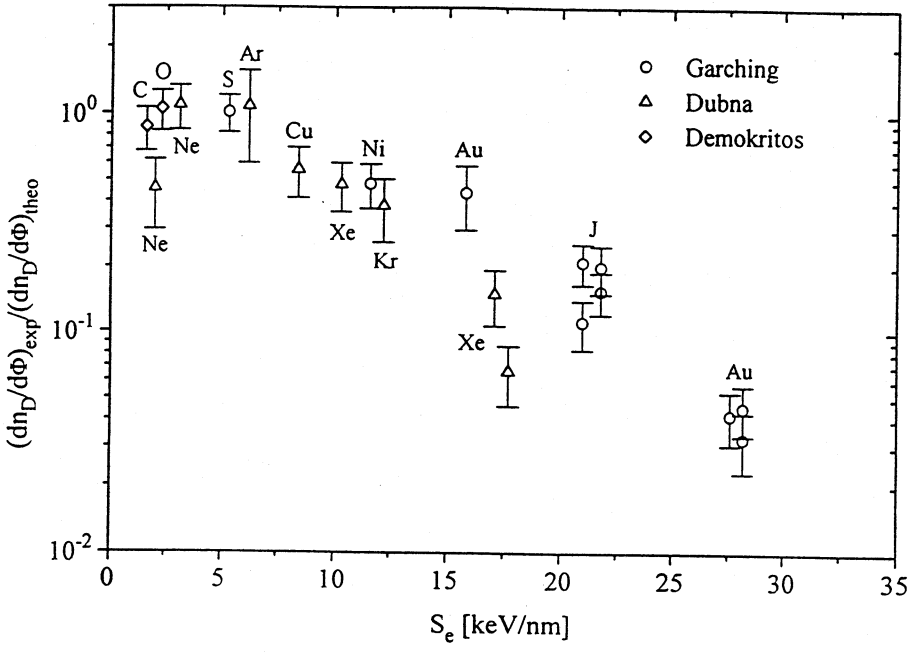

Fig.3. Systematics of the heavy-ion damaging efficiency as a function of the electronic stopping parameter for Ge. Normalized to unity for light ions.

Described above peculiarities correspond to the ion energy range near 1 MeV/u. At much lower energy, the ratio of electronic and nuclear stopping is changed significantly and one cannot expect similar processes of annealing in thermal spike. More probable that at the end of range the destructive effect of heavy ions should be enormous. The state of crystal medium in a deep layer can be studied by other methods, not by the detection of blocking pattern in situ under irradiation. Some interesting effects were revealed in Ref. [32] using the electron microscopy for the fractured Ge crystals exposed to the I and Au ion flux. In Fig.4, the cross-section SEM picture is shown for the Ge sample irradiated with 252 MeV Au ions up to fluence $4 \cdot 10^{15}$ ions/cm^2. This picture illustrates clearly the variety of crystal-response types dependent on the ion energy. At highest energies, near the surface a slightly damaged monocrystalline structure survives, the disordering is stronger at deeper layers, then, at some depth the matter is almost completely disordered being still dense, and near the end of ion range the stage of morphological instability is finally reached. Different forms are generated on the latter stage, as follows: chaotically distributed voids of different size inserted into an amorphized matter, regular sponge-like structure, and splitted slices of the material laterally extended by the normality to the beam. The morphological instability is the extreme of disordering and such stage can be reached in Ge only at high doses of low-energy ions as heavy as I and Au.

3. De-blocking and re-channeling

Within described above experimental scheme another series [24,25] was carried out on the irradiation of Si and Ge crystals with relatively light Ne, Al and Ar ions at higher energies up to 8

MeV/u. Again the scattered and recoiled nuclei were detected by solid state track detectors, but in this case not only the Rutherford scattering products were ejected from the target. The ratio of the elastic to nuclear inelastic yields can be estimated both for the projectile-like and target-like products, and this ratio depends strongly on the detection angle and energy. Finally, by choice of the detector type, the degrader-foil thickness at the top of detectors, and angle, it is possible to isolate for detection the specific product of interest. Then, the active layer thickness is to be calculated. At projectile energies in the range of (3-8) MeV/u, the active thickness can be increased up to 10 μm, while that is typically below 2 μm in experiments at 1 MeV/u (section 2).

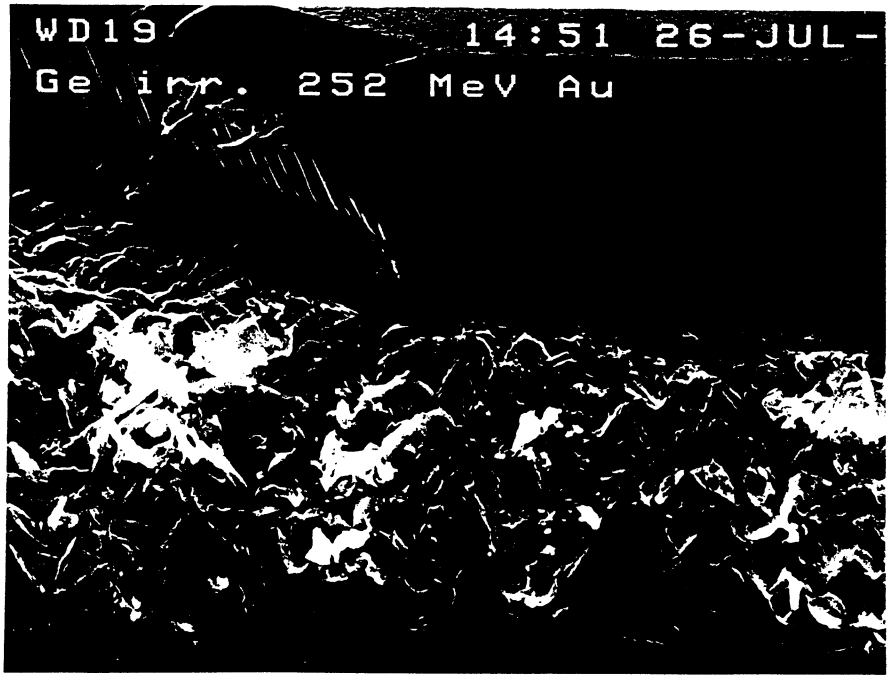

Fig.4. Cross-section SEM picture of a Ge sample exposed to the fluence of $4 \cdot 10^{15}$ Au ions/cm^2 at 252 MeV.

Very unusual transformation of the pattern character has been observed when the projectile energy is varied, or even at the same energy but at different angles to the beam. For illustration, the patterns detected at Ar + Si experiment are exhibited in Fig.5. One can see in Fig.5b that deep planar-blocking minima at some angles are degraded, and even are transformed to appear as channeling maxima. In Fig.6, the angular distributions near <111> Si axis are characterized quantitatively for different projectiles, energies and angles. The effect of deep-layer emission becomes evident. One has to mention that even 10 μm is much shorter than a total range of the light ions, and the fluence in experiment has been kept much lower than the strong damaging dose.

Analysis of experimental results [24,25] led to the following scenario explaining the transformation of blocking to channeling. At the emission point, where scattering or reaction is happened, the product is ejected from the nucleus ensconced in the lattice. Respectively, the blocking angular distribution is formed after a few nm path in crystal. This distribution is unstable because the randomizing multiple scattering processes are effective for de-blocking. Thus, the angular distribution

becomes to be isotropic after some path in crystal, like 5 μm thickness by estimation. On the residual path in crystal, the random distribution is rearranged once more due to the volume capture into channeling with corresponding peak along a crystallographic directory. This distribution is finally detected on the exit from crystal, see in Fig.5b. Especially strong channeling peaks are observed in the condition of "buried" source of particles emitted from the deep layer. Such case is realized, for instance, for 151 MeV Ar irradiation of Si at detection angles below 58°, as illustrated in Figs.5,6. The elastic scattering is suppressed at the near-surface layers, and only after degrading of the beam energy inside crystal, its cross-section grows up strongly and contributes the major part into the total yield of all particles at mentioned angles. This is nothing but a "buried" source of particles, and intense channeling peak corresponds to such condition.

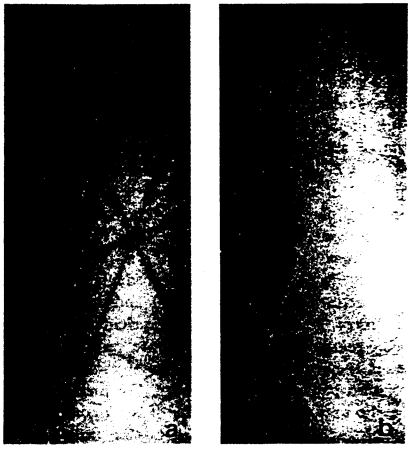

Fig.5. Reflection patterns recorded with glass detectors in Ar+Si irradiation at 25 MeV (a) and 151 MeV (b). Black lines correspond to planar blocking and light ones to channeling peaks.

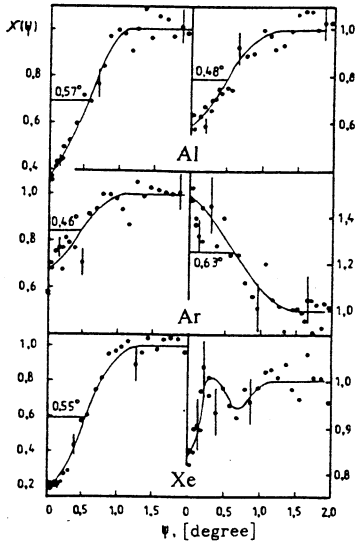

Fig.6. Angular distributions detected for <111> Si axis at experiments with Al, Ar and Xe beams. For Al the profiles shown correspond to the detection angle 64° and to the beam energies of 91 (left) and 148 (right) MeV; for Ar - 54°, 92 and 151 MeV; for Xe - 69° and 39°, 122 MeV, respectively.

The explanation above looks realistic in all respects, except it contradicts to the reversibility rule. Indeed, the directed transformation of angular distribution from blocking type to the isotropic one, and then to channeling type on the transmission through the crystal seems unusual. Especially surprising is the spontaneous formation of channeling peaks. After many discussions, the additional series of experiments was recognized to be necessary, and it is described in the following section.

4. Cooling and heating

In experiments [26-29] the transmission of wide-angle isotropic flux through monocrystalline foils has been studied. As a source of isotropic flux serves the beam scattering from specially installed polycrystalline target, or the α-radioactive source. A thin monocrystalline membrane stretched onto larger thickness frame has been kept out of the beam to avoid the damage of structure and the mechanical deformation of crystal. The following single crystals were available in a form of self-

supported foils: Si of 3 to 14 μm thickness, Ni – (1 to 4.5) μm, and Pt – (1 to 6) μm. The series of experiments with protons, α-particles and heavy ions were performed.

In Fig.7 the experimental scheme used for proton irradiation is shown. The beam of (0.5-1) MeV protons after diaphragms was scattered from thin gold target, and at backward direction, scattered protons were detected by CR-39 polymer track detector. The Si membrane was installed near the Au target out of the beam, and protons should transmit through the Si crystal on the way to the detector. The flux of scattered protons was practically isotropic within the frame of Si crystal. The crystallographic image (if appears) have to be recorded by the detector. In principle, the scheme was similar also in experiments with α-particles and heavy ions. Only the radioisotopic source was used in experiments with alphas instead of proton scattering target. At the case of heavy ions, the scattering to forward hemisphere was applied for increasing the flux of scattered particles, and the two-coordinate position sensitive ionization chamber was used as a detector. The glass track detectors were installed in some irradiations too.

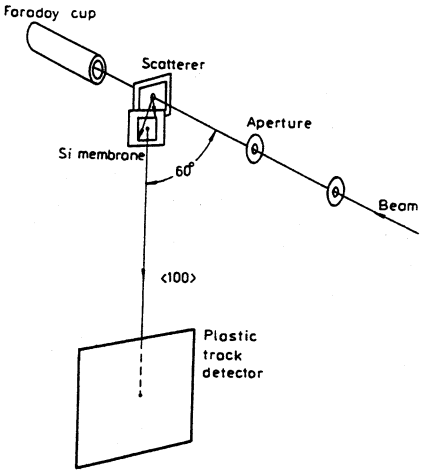

Fig.7. Schematic diagram of the setup in the experiment on proton transmission through Si

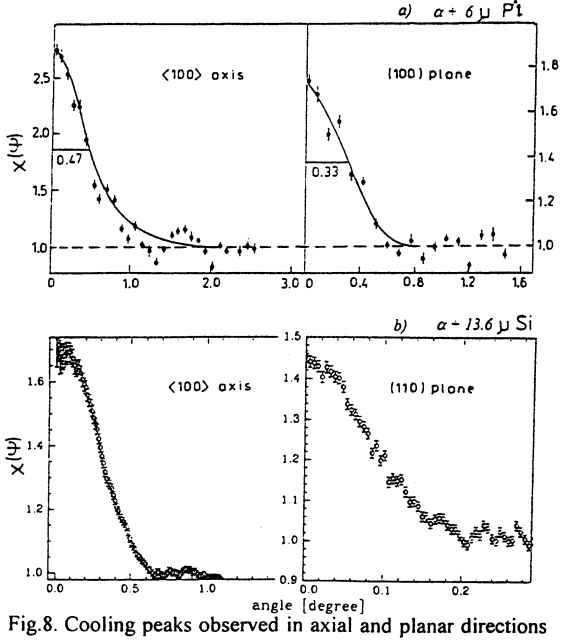

Fig.8. Cooling peaks observed in axial and planar directions for α-particles transmitted through crystals: a) 6 μm Pt and b) 13.6 μm Si. Final energy of detected alphas is 0.6 MeV in both cases.

Described series have been carried out at Ludwig-Maximilians University of München, and the Garching Tandem accelerator could supply beams of ions from O to Au for these experiments. The ionization chamber detector was precisely designed and provided a wide solid angle, high position and energy resolutions, plus the ΔE-signal used for particle identification. The detector system was previously calibrated in many experiments on the elastic recoil detection analysis ERDA, that ensured a reliable operation of the whole system. Procedure for the account of kinematics corrections in an authomatized manner was developed, as well as other software tools for the visualization of the two-coordinate images and the scanning of them. The solid state track detectors after etching were processes using the laser scanning system or the TV-installed microscope in order to quantify the coordinate (angular) dependence of the track density.

In experiments with (100) Si

crystal, the enhancement peaks along <100> axis and (011), (001) planes were clearly manifested both in the transmission of protons and α-particles. Being elementary particle, proton at low energy, within the range of (0.1-0.4) MeV can pick-up an electron, thus, hydrogen ions, the same as heavy ions, are influenced by the charge variation effects in medium. The enhancement profiles taken with Pt and Si crystals are compared in Fig.8 for the same energy (0.6 MeV) of α-particles after transmission through crystals. Stronger potential of the Pt lattice produces higher enhancement in comparison with Si. For protons and α-particles, the enhancement peak amplitude is decreasing and it almost disappears, when the output energy is increased and corresponds to the completely bare ion. The enhancement survives at low energies down to the lower limit defined by the detection threshold.

More complex behavior has been observed for heavy ions. The disappearance of the cooling peak at high energies could be observed only for C and O ions. The complete-stripping energy could not be reached for heavier ions because of the Tandem accelerator restrictions. For the medium-mass ions, the cooling peaks are observed at higher energy and the heating dips at lower energy. There is some transitional range of rather weak structure in angular distribution, and the transitional energy can be estimated using some conventional procedure. For example, such kind dependencies are shown in Fig.9 taken for Y ions in Si. Qualitatively similar behavior has been observed for many other ions, and not only in Si but also in Ni crystals.

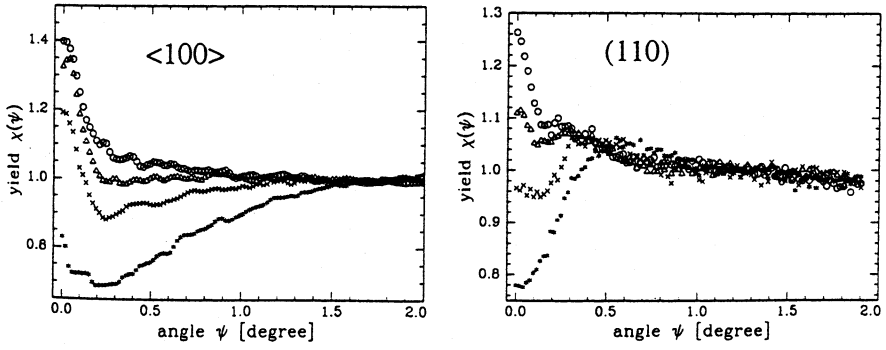

Fig.9. Axial and planar angular distributions of Y ions after transmission of a 3.4 μm Si (001) crystal. The exit energies are 141, 117, 92 and 63 MeV from the top to the bottom.

Ions lighter S show only the manifestation of the cooling peaks in Si, similarly to protons and alphas. Au ions, on the contrary, demonstrate only heating dips, but recently it was found that their energy at Garching accelerator was not enough for transition to cooling. At the GANIL experiment with 1 GeV Pb-ion beam, the cooling peaks are manifested after the transmission through Si crystal, and the transitional energy has been estimated, Ref. [33]. The systematics of the transitional energy values are discussed in Ref. [29]. All peculiarities described above are not yet well-understood, as well as the most surprising fact that the Pt crystal generates only cooling and no heating for all ions and energies. The discussion of cooling mechanism is given below.

5. Electron-capture and -loss model

As mentioned above, at some energy of light ions the cooling enhancement almost disappears, and such upper limits are pointed by arrows in Fig.10 taken from Ref. [27]. One can see the same position of the upper limit for H, He and C ions with respect to the corresponding curve of the electronic stopping, namely, near the energy where stopping begins to be E^{-1} dependent. Such a dependence corresponds to the stripping of last electron from the projectile, and consequently to the deterioration of the electron capture and loss. The cooling enhancement, thus, is correlated with the charge-exchange process, in accordance with the mechanism proposed in [26]. Its basic idea is the difference of the impact parameter dependence of electron capture and loss. If an ion captures an electron, its

potential energy is reduced, since the potential is in first approximation linearly proportional to the ion charge. This scheme is illustrated in Fig.11. A loss of an electron leads to a regain of transverse energy, which is smaller than the former reduction, if the electron loss happens further away from the atomic row of the crystal. Therefore, if the mean capture radius is smaller than the mean loss radius, a net transverse energy loss follows in a charge-exchange cycle, thus transverse cooling. If the two mean radii are reversed, a net transverse energy gain occurs, hence transverse heating.

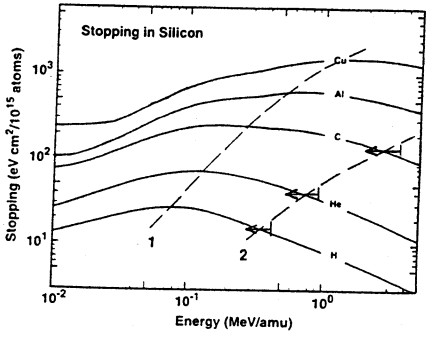

Fig.10. Standard energy-loss curves for ions in Si. The horizontal arrows indicate the range for observation of cooling effect in Si crystal for ^{1}H, ^{4}He and ^{12}C ions.

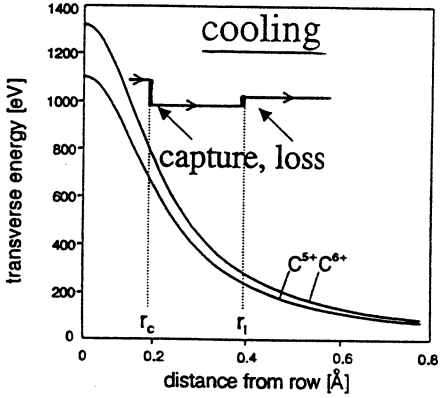

Fig.11. Illustration of the transverse potential energy change due to the electron capture and loss cycle for channeled C^{5+} and C^{6+} ions.

The classical estimates of the two radii in [26] give more or less satisfying results, while the calculation [34] within Born-approximation yields a rather small electron capture radius. But even more important disadvantage of such model looks as follows: the appearance of cooling or heating at any real condition is just translated through this model to the mean radii of capture and loss. Independent calculations of such parameters, especially for very heavy ions as a function of the ion velocity is almost impossible at the modern status of the numerical calculations. So that, for the development of interpretation the possibility remains to establish some empirical regularities by experimental results and to understand them. In Ref. [27], we already discussed the role of free path lengths for electron capture and loss and importance of their comparison with the crystal thickness and with the wavelength of the channeling trajectory. More theoretical approach is given in Ref. [30] for the analysis of the spatially correlated charge-exchange events as a reason for the reversibility violation.

Measured angular distributions demonstrate the dependence on the crystal and ion species, final energy of transmitted ion, crystal thickness and Miller indexes of a crystallographic direction. Among the dependencies, one might distinguish the regular manifestations, and some of them could be understood even without the microscopic mechanism clarifying. Some regularities can be listed as follows:

1. Growth of the enhancement with the crystal thickness, t. This is understood as integration of the effect due to multiple electron capture-loss events. The decrease of the transverse energy is accumulated with the growth of the number of elementary events. The latter number can be estimated roughly as a ratio $t/\ell_{capt.}$, where $\ell_{capt.}$ is the free-path length of the ion for the electron capture process.
2. At large thickness, the enhancement peak becomes to be high in amplitude, and it is typically narrow, the angular width is lower than the Lindhard angle. It could be explained assuming that the total number of particles in the peak is conserved, and the growth of amplitude means decrease of the width.

3. The angular width of the heating minimum is typically larger than the Lindhad angle, while the cooling peak is narrower.
4. Oscillations in the angular dependence are often manifested. When the central peak has low amplitude, the amplitude of the oscillations can be comparable with the maximum of the peak. One may try to explain them by the quantum levels of the transverse energy in the potential well, but the estimations show a high level density, and support a rather classical interpretation.
5. It was observed that different planes sometimes show very different behavior. Not only the peak amplitude, but the type of pattern is changed being a peak for stronger plane and a dip for weaker. That was detected in some cases of heavy-ion transmission through Si, when (110) – strong and (100) – weak planes are compared. Within the model of charge-exchange the magnitude of ratio between mean radii of capture $\rho_{capt.}$ and loss ρ_{loss} is important. The ratios of both radii to half the interplane spacing, $d_p/2$ are also important. For the weaker plane with narrower planar channels, both capture and loss radii at some energy reach a value close to $d_p/2$, and in this situation the heating may appear easy. The observation of qualitatively different profiles for the (110) and (100) planes, probably, corresponds to such a case.
6. Cooling enhancement is observed in Si and Pt crystals as well, although the physical parameters of both crystals are very different. For instance, the electron density and linear energy losses are much higher in Pt. By estimation, the mean path-length for electron-loss, ℓ_{loss} should be 3 times shorter in Pt, than is Si. As discussed in Ref. [27], for effective cooling, ℓ_{loss} should not be much shorter than $\lambda/4$ – quarter of the channeling-trajectory wavelength. And it would be interesting to find that λ is also 3 times shorter in Pt, than is Si, because of stronger lallice potential. Finally, the ratio between ℓ_{loss} and $\lambda/4$ remains almost the same for Pt and Si, and the charge-exchange cooling mechanism works well in both crystals.

One remark at the end: the developed Monte Carlo codes describing the ion transmission through crystal as a sequence of binary collisions do not reproduce the cooling and heating effects until the special assumptions are inserted on different impact-parameter dependencies of capture and loss cross-sections. This has been shown using the Crystal TRIM [35] and UPIC [36] codes.

Summary

The series of experiments have been carried out for the investigation of a crystal response to the irradiation with very heavy ions and the effects of a particle flux rearrangement under transmission. The defect annealing is found to be a consequence of the thermal spike creation in semiconducting crystals after a transmission of very heavy ion at an energy of about 1 MeV/u. When an energy is decreased at the deep layers, the crystal ordering is drastically changed, and the stages of the amorphization and morphological instability can be reached.

The flux redistribution of ions in crystals has been studied and the violation of reversibility rule is established after the observation of different manifestations. In particular, the transformation of blocking to channeling for particles emitted from a deep layer has been found in the series of reflection-geometry experiments. On the transmission of isotropic flux through crystals, the crystallographic structures have been observed in a form of enhancement or reduction of the flux near the directions of axes and planes. So that, the transverse cooling or heating are both possible, and the conditions for the transition from cooling to heating are investigated. For many ions in Si and Ni crystals such a transition takes place at definite energies. Other parameter dependencies of cooling and heating have also been obtained and discussed for qualitative understanding. The mechanism of electron capture and loss might be useful, but an adequate, suitable model of cooling and heating was not yet developed.

References

1. G.H. Kinchin, and R.S. Pease, Rep. Progr. Phys. 18 (1955) 1.
2. R.L. Fleischer, P.B. Price, and R.M. Walker, J. Appl. Phys. 36 (1965) 3645.
3. R. Katz et al, Rad. Eff. Def. Solids, 114 (1990) 15.

4. C. Watson, and T. Tombrello, Rad. Eff. 89 (1985) 263.
5. I.A. Baranov et al, Uspekhi Fiz. Nauk, 156 (1988) 477.
6. M. Toulemonde, C. Duffour, E. Paumier, Phys. Rev. B46 (1992) 14362.
7. G. Szenes, Mater. Sci. Forum, 97-99 (1992) 647.
8. S.A. Karamyan, Rad. Meas., 25 (1995) 125.
9. E.M. Bringa, and R.E. Johnson, Phys. Rev. Lett. 88 (2002) 165501.
10. S.A. Karamyan, Yu.Ts. Oganessian, V.N. Bugrov, Nucl. Instr. Meth. B43 (1989) 153.
11. S.A. Karamyan, Nucl. Instr. Meth. B51 (1990) 354.
12. W. Assmann et al, Nucl. Instr. Meth. B146 (1998) 271.
13. S. Furuno et al, Nucl. Instr. Meth. B107 (1996) 223.
14. A. Dunlop, D. Lesueur, and J. Dural, Nucl. Instr. Meth. B42 (1989) 182.
15. A. Iwase et al, Phys. Rev. Lett. 58 (1987) 2450.
16. S. Klaumüntzer, G. Schumacher, Phys. Rev. Lett. 51 (1983) 1987.
17. J. Stark, Z. Phys. 13 (1912) 973.
18. P.B. Treacy, Austral. J. Sci. 22 (1960) 334.
19. M.M. Bredov, and I.M. Okuneva, Sov. Phys. Dokl. 113 (1957) 795.
20. W.M. Gibson, Ann. Rev. Nucl. Sci. 25 (1975) 465.
21. J. Lindhard, Mat. Fyz. Medd. Dan. Vid. Selsk. 34 (1965) No.14.
22. V.V. Beloshitsky, and M.A. Kumakhov, Sov. Phys. JETP 39 (1974) 876.
23. R.W. Fearick, Nucl. Instr. Meth. B193 (2002) 139.
24. S.A. Karamyan, Izv. Akad. Nauk SSSR, Ser. Fiz. 51 (1987) 1008.
25. S.A. Karamyan, Yad. Fiz. 49 (1989) 934.
26. W. Assmann, H. Huber, S.A. Karamyan et al, Phys. Rev. Lett. 83 (1999) 1759.
27. S.A. Karamyan et al, Nucl. Instr. Meth. B164-165 (2000) 61.
28. S.A. Karamyan et al, Nucl. Instr. Meth. B193 (2002) 144.
29. F. Grüner et al, Nucl. Instr. Meth. B193 (2002) 165.
30. J.U. Andersen et al, Nucl. Instr. Meth. B193 (2002) 118.
31. H. Huber, W. Assmann, S.A. Karamyan et al, Nucl. Instr. Meth. B146 (1998) 309.
32. H. Huber, W. Assmann, S.A. Karamyan et al, Nucl. Instr. Meth. B122 (1997) 542.
33. F. Grüner, W. Assmann, S.A. Karamyan et al, Report on the May, 2002 experiment at GANIL. Unpublished.
34. D.H. Jakubassa-Amundsen, Phys. Rev. B65 (2002) 174110.
35. M. Posselt, Rad. Eff. Def. in Solids. 130/131 (1994) 87.
36. V.A. Khodyrev, V.Ya. Chumanov, G.P. Pokhil and K.K.Bourdelle, Nucl. Instr. Meth. B94 (1994) 523.

Received on February 6, 2003.

Карамян С. А., Грюнер Ф., Ассманн В.
E14-2003-24

Охлаждение и нагрев потока ионов
при прохождении через кристаллы

Прохождение заряженных частиц через монокристаллическую среду сопровождается многими интересными явлениями. В настоящей работе описано одно из новых недавно обнаруженных и экспериментально исследованных явлений — перераспределение изотропного потока. В результате модификации траекторий прохождения под действием кристалла происходит охлаждение или нагрев в координате поперечного импульса. Это означает нарушение правила обратимости и не объясняется традиционной теорией каналирования. Тип наблюдаемого изображения (усиление или ослабление) и его интенсивность зависят от сорта ионов и кристалла, от энергии ионов и толщины кристалла. Такие зависимости изучены экспериментально. Для объяснения привлекается механизм, включающий регулярную последовательность событий перезарядки, которые приводят к несохранению поперечной энергии. Дан также обзор и приведены оригинальные результаты по проблеме отклика кристаллической среды на прохождение потока ионов.

Работа выполнена в Лаборатории ядерных реакций им. Г. Н. Флерова ОИЯИ.

Препринт Объединенного института ядерных исследований. Дубна, 2003

Karamyan S. A., Grüner F., Assmann W.
E14-2003-24

Cooling and Heating of the Ion Flux
on the Transmission through Crystals

Transmission of charged particles through a monocrystalline medium is accompanied by many interesting phenomena, and a new one — redistribution of the isotropic flux — is now studied experimentally and described in the present work. The cooling or heating in the transverse momentum coordinate arises as a result of crystal-induced modification of the transmission trajectories. This indicates the violation of the reversibility rule, and cannot be explained within prevailing theory of channeling. The type of image (enhancement or reduction) and its intensity are dependent on the ion and crystal species, on an energy of ions and on the crystal thickness. Such dependencies have been studied experimentally and the mechanism involving the regular sequence of charge-exchange events with the transverse-energy non-conservation is attracted for understanding. The crystal response to ion flux transmission is also reviewed and characterized by the original results.

The investigation has been performed at the Flerov Laboratory of Nuclear Reactions, JINR.

Preprint of the Joint Institute for Nuclear Research. Dubna, 2003

Макет *Т. Е. Попеко*

Подписано в печать 28.02.2003.
Формат 60 × 90/16. Бумага офсетная. Печать офсетная.
Усл. печ. л. 0,93. Уч.-изд. л. 2,04. Тираж 280 экз. Заказ № 53792.

Издательский отдел Объединенного института ядерных исследований
141980, г. Дубна, Московская обл., ул. Жолио-Кюри, 6.
E-mail: publish@pds.jinr.ru
www.jinr.ru/publish/